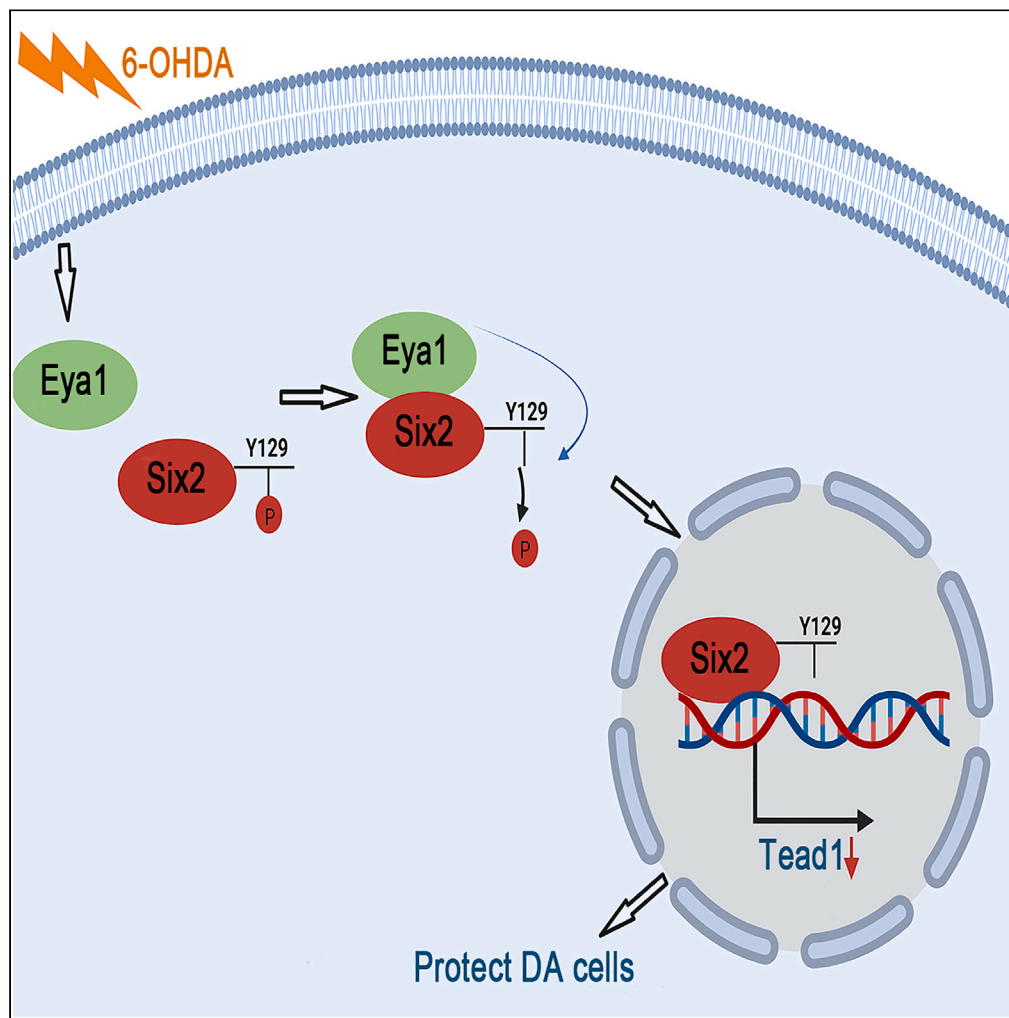


Article

Dephosphorylation of Six2Y129 protects tyrosine hydroxylase-positive cells in SNpc by regulating TEA domain 1 expression



Can-tang Zhang,
Deng-li Qin, Xia-
yin Cao, Jia-shuo
Kan, Xin-xing
Huang, Dian-shuai
Gao, Jin Gao

gaojin@xzhmu.edu.cn

Highlights

Six2Y129 site was
dephosphorylated by
phosphatase Eya1 in
injured DA cells

Dephosphorylated Six2
translocated from
cytoplasm to nucleus

Dephosphorylated Six2
protected DA cells by
down-regulating Tead1
expression

Zhang et al., iScience 26,
107049
July 21, 2023 © 2023 The
Authors.
[https://doi.org/10.1016/
j.isci.2023.107049](https://doi.org/10.1016/j.isci.2023.107049)

Article

Dephosphorylation of Six2Y129 protects tyrosine hydroxylase-positive cells in SNpc by regulating TEA domain 1 expression

Can-tang Zhang,¹ Deng-li Qin,² Xia-yin Cao,² Jia-shuo Kan,² Xin-xing Huang,² Dian-shuai Gao,² and Jin Gao^{2,3,*}

SUMMARY

Parkinson's disease (PD) is a neurodegenerative disease characterized by selective loss of dopaminergic (DA) neurons in the substantia nigra pars compacta (SNpc). We recently reported that Six2 could reverse the degeneration of DA neurons in a dephosphorylation state. Here we further identified that Eya1 was the phosphatase of Six2 that could dephosphorylate the tyrosine 129 (Y129) site by forming a complex with Six2 in damaged DA cells. Dephosphorylated Six2 then translocates from the cytoplasm to the nucleus. Using ChIP-qPCR and dual luciferase assay, we found that dephosphorylated Six2 down-regulates TEA domain1 (Tea1) expression, thus inhibiting 6-hydroxydopamine (6-OHDA)-induced apoptosis in DA cells. Furthermore, we showed Six2Y129F/Tea1 signaling could protect against the loss of SNpc tyrosine hydroxylase-positive (TH⁺) cells and improve motor function in PD model rats. Our results demonstrate a dephosphorylation-dependent mechanism of Six2 that restores the degeneration of DA neurons, which could represent a potential therapeutic target for PD.

INTRODUCTION

Parkinson's disease (PD) is the second most common neurodegenerative disorder and is characterized by the selective loss of dopaminergic (DA) neurons in the substantia nigra pars compacta (SNpc). The main symptoms of PD are movement disorder which includes tremors, rigidity, bradykinesia, and postural instability. Currently, drugs for PD management are either complementing or mimicking endogenous dopamine. Although these treatments can relieve symptoms, they cannot stop or reverse the progression of the disease. Therefore, the most significant challenge remains to develop treatments that protect and restore DA neurons.^{1–3}

The Sineoculis homeobox homolog 2 (Six2) transcription factor is a member of the SIX family, which belongs to the homeobox gene superfamily. To date, six family genes have been identified in various species ranging from lower invertebrates, including nematodes to higher mammals, such as humans. There are six members classified into three groups, Six1/Six2, Six3/Six6, and Six4/Six5, which are characterized by a six-type homeodomain (HD, 60 amino acids) and a six-type domain (SD, 110–115 amino acids).^{4,5} Extensive studies have focused on the role of Six family protein control in cell proliferation, differentiation, and cell fate determination.^{6–8} However, some recent findings suggested they also play an essential role in cell apoptosis.^{9,10} Our previous work showed that Six2 could mediate the anti-apoptotic function of the glial cell line-derived neurotrophic factor on DA neurons by regulating smurf1 expression.¹¹ In addition, we also observed that Six2 exerted its anti-apoptotic effect under the dephosphorylated state.¹² However, which phosphatase regulates its dephosphorylation and the dephosphorylated sites of Six2 still need to be clarified.

Eyes absent homolog1 (Eya1), a member of the Eya gene family, is a transcriptional co-activator with intrinsic protein phosphatase activity. All mammalian Eya proteins contain a highly conserved C-terminal Eya domain, which interacts with Six transcription factors, and a less conserved N-terminal Eya domain.^{13,14} Like members of the Six family, Eya proteins are critical to multiple organ development, in part by acting on Six proteins to promote the proliferation and survival of progenitor cell populations.^{15–18} Structurally, Eya proteins belong to the halogenated acid dehalogenase superfamily¹⁹ and have dual protein tyrosine (Y) as well as threonine (T) phosphatase activity.^{20–23} So far, only five active substrates of eya tyrosine

¹Department of Respiratory and Critical Care, the Affiliated Hospital of Xuzhou Medical University, Xuzhou, Jiangsu 221004, China

²Department of Neurobiology and Cell Biology, Xuzhou Key Laboratory of Neurobiology, Xuzhou Medical University, Xuzhou, Jiangsu 221004, China

³Lead contact

*Correspondence: gaojin@xzhmu.edu.cn
<https://doi.org/10.1016/j.isci.2023.107049>



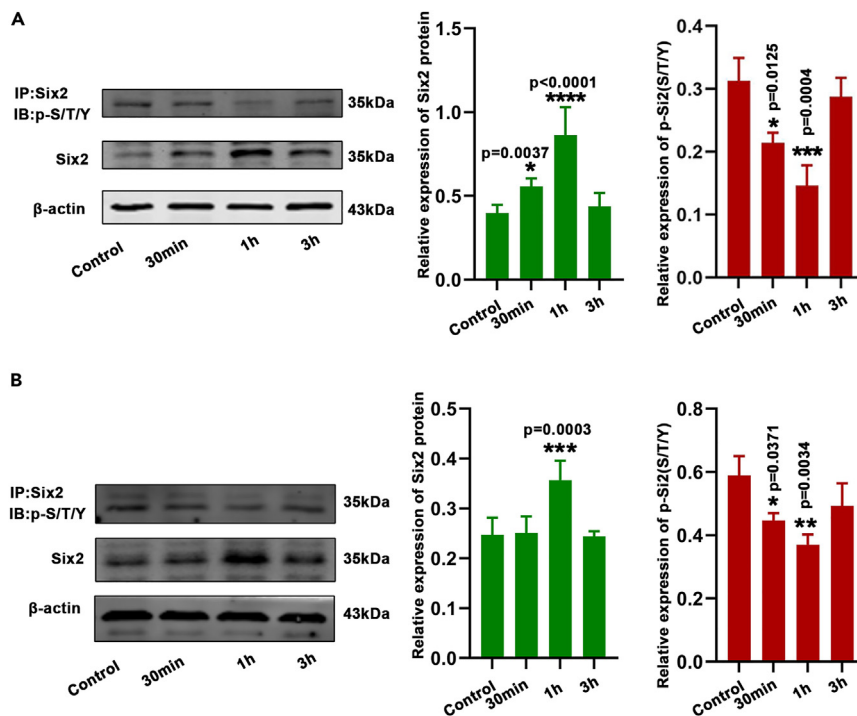


Figure 1. Changes of Six2 phosphorylation level in dopaminergic (DA) cells injured by 6-hydroxydopamine (6-OHDA)

(A) Changes and statistical analysis of Six2 and phosphorylated Six2 level in MES23.5 cells after treatment with 6-OHDA (100 μ M) for 30 min, 1h, and 3h.

(B) Changes and statistical analysis of Six2 and phosphorylated Six2 level in MN9D cells after treatment with 6-OHDA (100 μ M) for 30 min, 1h, and 3h. The statistical analysis was carried out using one-way ANOVA followed by *post hoc* Dunnett's tests. * $p < 0.05$, ** $p < 0.01$, *** $p < 0.001$ and **** $p < 0.0001$; $n = 3$; p-S/T/Y: phosphoserine/threonine/tyrosine.

phosphatase have been identified, and they are the DNA damage-related histone H2AX,^{24,25} the β -form of the estrogen receptor (ER β),²⁶ the proto-oncogene Myc,²³ the Notch1²⁷ and atypical protein kinase C (aPKC),²⁸ as well as other potential substrates have been proposed.²⁹ Some studies have demonstrated that EYA and SIX proteins function as transcriptional activation complexes and play essential roles in organogenesis during development and disease.³⁰ In previous work, we documented that knockdown of Eya1 significantly increased Six2 phosphorylation levels in DA neurons at the early stage of the injury.¹² However, it is unclear whether Eya1 is the phosphatase of Six2.

In this study, we identified that Eya1 was the phosphatase of Six2 and could dephosphorylate the tyrosine 129 (Y129) site of Six2 by forming a complex with Six2 in injured DA cells. Then the dephosphorylated Six2 translocated from the cytoplasm to the nucleus and directly inhibited the expression of Tead1, antagonizing the apoptosis of DA neurons and improving motor function in PD rats. This study will provide a theoretical target for drug development to halt or reverse the progressive degeneration of DA neurons in PD.

RESULTS

Six2 is dephosphorylated in damaged MES23.5 DA cells

To investigate whether the phosphorylation level of Six2 decreased in injured DA cells, we cultured MES23.5 and MN9D DA cells and treated them with 6-OHDA for 30 min, 1 h, and 3 h, respectively. IB analysis showed that the protein expression of Six2 increased in MES23.5 DA cells compared with control groups, especially at 1 h after 6-OHDA treatment. However, the serine/threonine/tyrosine (S/T/Y) amino acid phosphorylation level of Six2 decreased significantly at 1 h after 6-OHDA treatment (Figure 1A). The changing trend of Six2 and p-Six2 in MN9D cells treated with 6-OHDA was similar to that in MES23.5 cells. However, the changing trend was more evident in MES23.5 cells (Figure 1B).

Six2 is dephosphorylated by Eya1 in damaged MES23.5 DA cells

Our previous work has shown that overexpression of Eya1 could reduce the phosphorylation level of Six2 in injured DA cells.¹² To assess whether Eya1 is the phosphatase of Six2, we first evaluated the possibility of the interaction between the two proteins. IF results showed that both Eya1 and Six2 were co-expressed in MES23.5 DA cells (Figure 2A). Co-IP analysis using extracts from MES23.5 DA cells showed evident interaction between Eya1 and Six2 in control groups (Figure 2B); however, a weaker interaction between the two proteins was detected in DA cells treated with 6-OHDA for 1 h (Figure 2C). And further GST-pull-down analysis using extracts from 293T cells transfected with GST-Eya1/Six2 confirmed that Eya1 could form a complex with Six2 directly (Figures 2D and 2E).

Next, we tested whether the interaction between Eya1 and Six2 could represent an enzyme-substrate relationship. We co-expressed Eya1/Six2 and Eya1D327A/Six2 in MES23.5 DA cells because the 327D site is essential for its phosphorylase activity. Results showed that the expression of Eya1, Eya1D327A, and Six2 increased in overexpressed groups than in control groups (Figures 2F and 2H). Moreover, the phosphorylation level of Six2 has dramatically upregulated in the phosphatase inactive mutant Eya1D327A group compared with the wild-type group in injured DA cells (Figure 2I). Because current evidence suggests that Eya1 is a tyrosine and threonine-specific phosphatase, we evaluated whether Eya1 functions as a tyrosine or threonine phosphatase on Six2 in injured DA cells. Results showed that the phosphotyrosine level of Six2 decreased clearly. In contrast, phosphothreonine level had no change compared with the control group in DA cells treated with 6-OHDA for 1h (Figure 2J). Taken together, phosphatase Eya1 could form a complex with Six2 and dephosphorylate the tyrosine of Six2 in DA cells treated with 6-OHDA.

Six2Y129 site was dephosphorylated by Eya1 in injured DA cells

We next sought to identify precisely which tyrosine residue(s) on Six2 were phosphorylated. Mutagenesis of each of the six tyrosine residues of phenylalanine (F) in Six2, including Y67F, Y92F, Y109F, Y129F, Y143F, and Y148F, were expressed in MES23.5 DA cells (Figure 3A). IB analysis revealed that only mutation of tyrosine residue 129 blocked Six2 tyrosine phosphorylation compared with other mutant and wild-type Six2 groups (Figure 3B), indicating that Y129 was the phosphorylated tyrosine.

Furthermore, mutants of tyrosine residue 129 to aspartic acid (D) of Six2 (Six2Y129D) were co-expressed with Eya1 in MES23.5 DA cells (Figure 3C). Then these cells were treated with 6-OHDA, IB analysis showed that the wild-type Six2 group displayed a loss of tyrosine phosphorylation in response to 6-OHDA, Six2Y129F overexpressed cells also significantly decreased tyrosine phosphorylation levels, whereas tyrosine phosphorylation levels of Six2Y129D groups did not affect compared with the Six2 groups (Figure 3D). These results indicate that Y129 is the dephosphorylated site of Six2 in damaged DA cells, and we further confirmed this view by *in vitro* phosphatase analysis. The immunopurified His-fusion wild-type Eya1 and its mutant Eya1D327A were mixed with Six2-pY129 peptides, and the results of phosphatase analysis showed that wild-type Eya1 effectively removed the phosphate group from Six2, whereas the phosphatase-inactive mutant Eya1D327A proteins had little or no effect (Figure 3E), we also used the known substrate H2AX of Eya1 as a positive control (Figure 3F). These data establish the ability of Eya1 to dephosphorylate the Y129 site of Six2 directly.

Dephosphorylated Six2 translocated from cytoplasm to nucleus

In the above results, we have shown a weaker interaction between Eya1 and Six2 proteins in DA cells after treatment with 6-OHDA (Figure 2B). To explore the reason why the binding of the two proteins becomes weaker, we further detected the distribution of Eya1 and Six2 in DA cells using laser confocal analysis. Results showed that both Eya1 and Six2 primarily distributed in the cytoplasm in control cells, however, Six2 translocated from the cytoplasm to the nucleus after 6-OHDA treatment, whereas Eya1 still located mainly in the cytoplasm (Figure 4A). These results of laser confocal indicate that maybe the phosphorylation state of Six2 affects its localization in DA cells. We further overexpressed Six2Y129F and Six2Y129D mutants in DA cells, respectively. Laser confocal results showed that Six2Y129F was mainly localized in the nucleus, whereas Six2Y129D was primarily located in the cytoplasm even after 6-OHDA treatment (Figure 4B). Then, we detected the expression of wild-type and mutants of Six2 in cytoplasm and nucleus by IB analysis. Results indicated that the expression of Six2 in the cytoplasm was higher than that in the nucleus, whereas Six2Y129F was mainly expressed in the nucleus in untreated MES23.5 cells. However, after treatment with 6-OHDA, the Six2 protein in the nucleus was significantly higher than that in the cytoplasm, whereas Six2Y129D was primarily expressed in the cytoplasm (Figure 4C). These data suggest that the dephosphorylation of Six2Y129 is essential for its translocation from the cytoplasm to the nucleus.

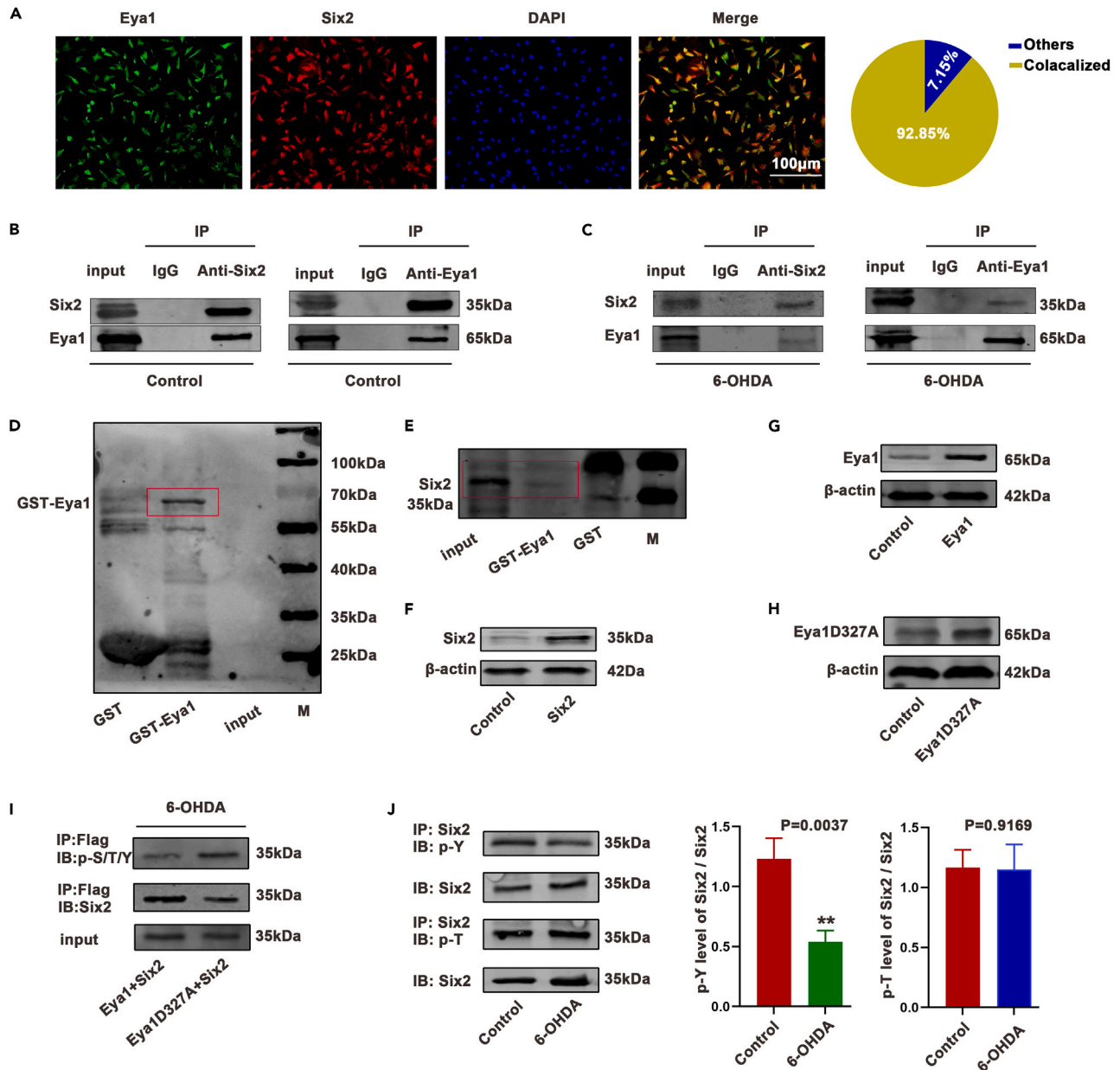


Figure 2. Six2 is dephosphorylated by Eya1 in damaged MES23.5 DA cells

(A) Immunofluorescence analysis detects the co-expression of Eya1 and Six2 in MES23.5 DA cells. The yellow color in the pie chart represents the percentage of cells colocalized by Eya1 and Six2 in total cells, and blue shows the percentage of cells without significant co-localization in total cells, n = 4.

(B and C) Co-immunoprecipitation (Co-IP) analysis evaluates the interaction between Eya1 and Six2 in control cells and cells treated with 6-OHDA (100 μM) for 1 h.

(D) The expression of GST-Eya1 in cultured 293T cells.

(E) GST-pull down analysis detects the direct interaction between GST-Eya1 and Six2 proteins in 293T cells.

(F) The expression of Six2 in cultured DA cells.

(G) The expression of Eya1 in cultured DA cells.

(H) The expression of Eya1D327A in cultured DA cells, D: aspartic acid; A: alanine.

(I) The effect of phosphorylase inactivation of Eya1(Eya1D327A) on the phosphorylation level of Six2 in cultured MES23.5 DA cells.

(J) IP coupled with IB analysis show the phosphotyrosine (pY) level and phosphotherosine (pT) level of Six2 in MES23.5 DA cells treated with 6-OHDA for 1 h. The statistical analysis was carried out using t tests. *p < 0.05; n = 3.

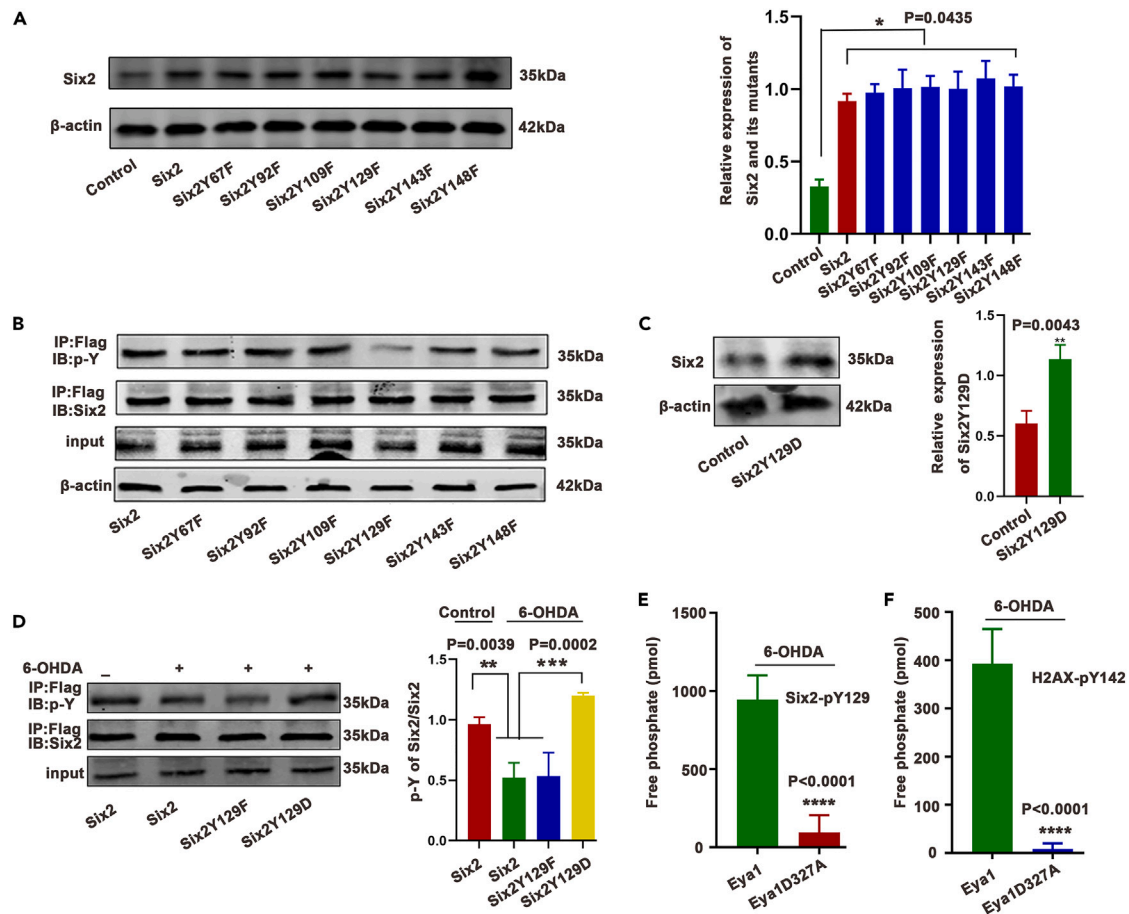


Figure 3. Six2Y129 site was dephosphorylated by Eya1 in injured DA cells

(A) IB analysis detect the over-expression of wild type and mutagenesis of Six2 (Y67F, Y92F, Y109F, Y129F, Y143F, and Y148F) in MES23.5 DA cells, Y: tyrosine; F: phenylalanine.

(B) IP coupled with IB analysis showed the phosphotyrosine level of Six2 and its mutagenesis (Y67F, Y92F, Y109F, Y129F, Y143F, and Y148F) in MES23.5 DA cells.

(C) IB analysis detected the over-expression of wild type and mutagenesis of Six2 (Y129D) in MES23.5 DA cells.

(D) IP coupled with IB analysis showed the phosphotyrosine level of Six2 and its mutants (Y129F and Y129D) in MES23.5 DA cells treated with 6-OHDA for 1 h.

(E) *In vitro* phosphatase analysis to evaluate whether Eya1 is the phosphorylase of Six2.

(F) Positive control of Six2 using the known substrate H2AX of Eya1. The statistical analysis was carried out using t tests, one-way ANOVA followed by post hoc Newman–Keuls tests, and one-way ANOVA followed by post hoc Dunnett’s tests. ** $p < 0.01$, *** $p < 0.001$ and **** $p < 0.0001$; $n = 3$.

Dephosphorylated Six2 regulates the expression of Tead1 in injured DA cells

The primary function of transcription factors is to regulate gene expression. Our results demonstrated that dephosphorylated Six2 could translocate into the nucleus from the cytoplasm. For an unbiased assessment of the plausible mechanisms of Six2, we performed a genome-wide ChIP-seq analysis for Six2 in MES23.5 DA cells. The ChIP-seq data presented differentially expressed genes between DA cells treated with the 6-OHDA and control groups. Of the Six2-binding sites, 14.63% were located in the region of 2000 bp upstream from the transcription start site of the differential genes (Figure 5A). The Gene Ontology (GO) analysis showed that the genes participated in the biological processes (Figure 5B). Meanwhile, the Kyoto Encyclopedia of Genes and Genomes (KEGG) analyses showed that the gene expression levels in Hippo pathways significantly differed between the two groups (Figure 5C). We also performed *de novo* motif discovery to identify specific sequences bound by Six2 (Figure 5D). We then detected the expression levels of TEA domain1 (Tead1) involved in Hippo pathways using qRT-PCR. The results showed that the mRNA expression level of Tead1 was significantly downregulated after 6-OHDA treatment (Figure 5E). Double luciferase reporter gene analysis showed that Six2Y129F mutants significantly inhibited the transcriptional activity of *Tead1* compared with the wild-type Six2 group in DA

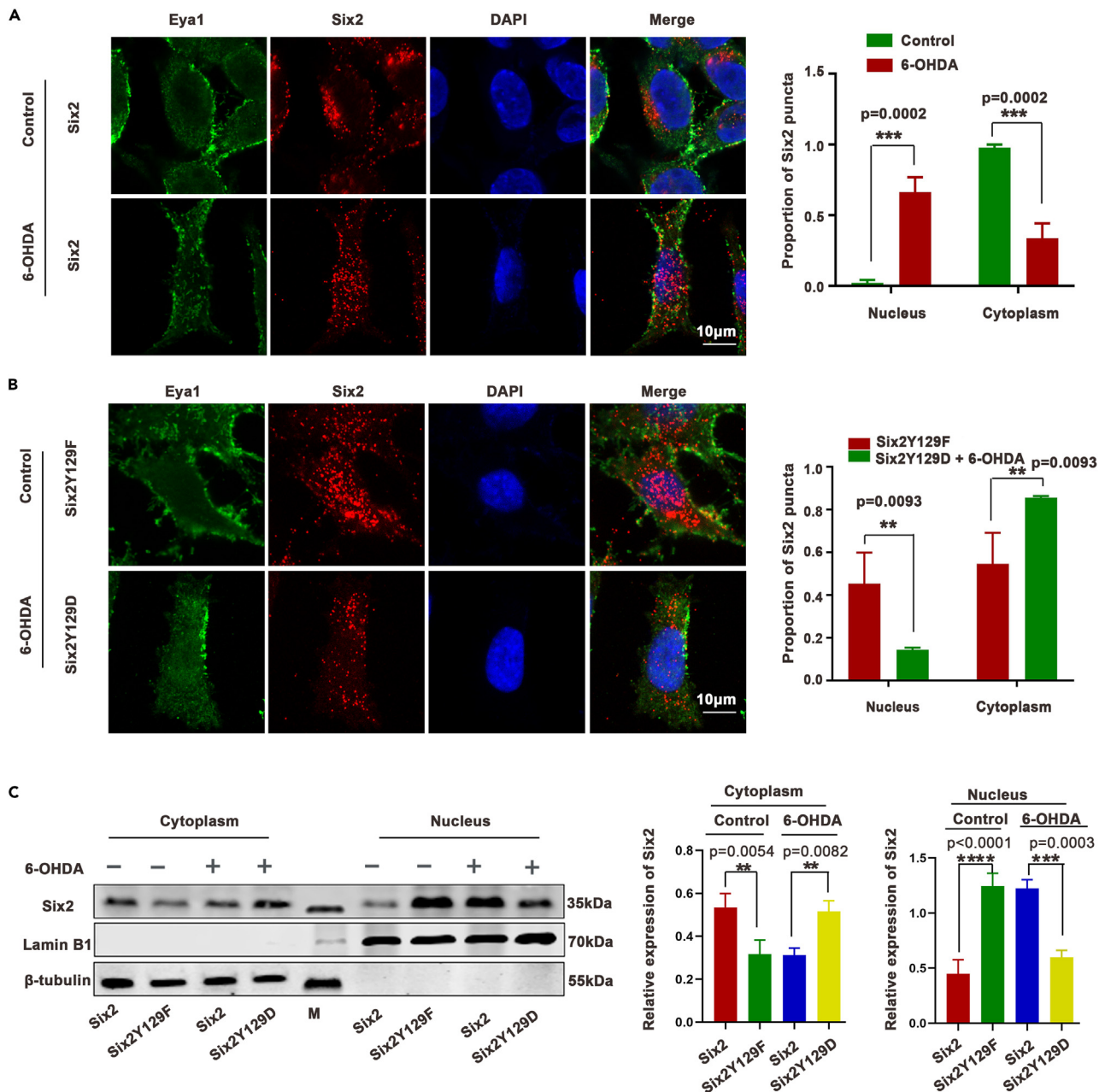


Figure 4. Dephosphorylated Six2 translocated from cytoplasm to nucleus in injured MES23.5 cells

(A) Laser confocal analysis detects the localization of Eya1 and Six2 in untreated MES23.5 DA cells and cells treated with 6-OHDA for 1 h. The proportion of Six2 puncta in cytoplasm and nucleus was analyzed by ImageJ, n = 4.

(B) Laser confocal analysis detects the localization of Eya1 and mutants of Six2 (Six2Y129F and Six2Y129D) in control and cells treated with 6-OHDA for 1 h. The proportion of Six2 puncta in cytoplasm and nucleus was analyzed by ImageJ, n = 4.

(C) IB analysis detects the expression of wild-type and mutants of Six2 (Six2Y129F and Six2Y129D) in cytoplasm and nucleus in control and 6-OHDA treated cells. The statistical analysis was carried out using t tests. *p < 0.05, **p < 0.01; n = 3.

cells treated with 6-OHDA, in contrast, Six2Y129D mutants significantly enhanced the transcriptional activity (Figure 5F). ChIP-qPCR results also showed that the binding ability of Six2Y129F to the *Tead1* promoter region increased compared with the Six2 group, whereas the binding ability of Six2Y129D decreased (Figure 5G). These results suggest that dephosphorylated Six2 negatively regulates the expression of *Tead1* by binding to its promoter.

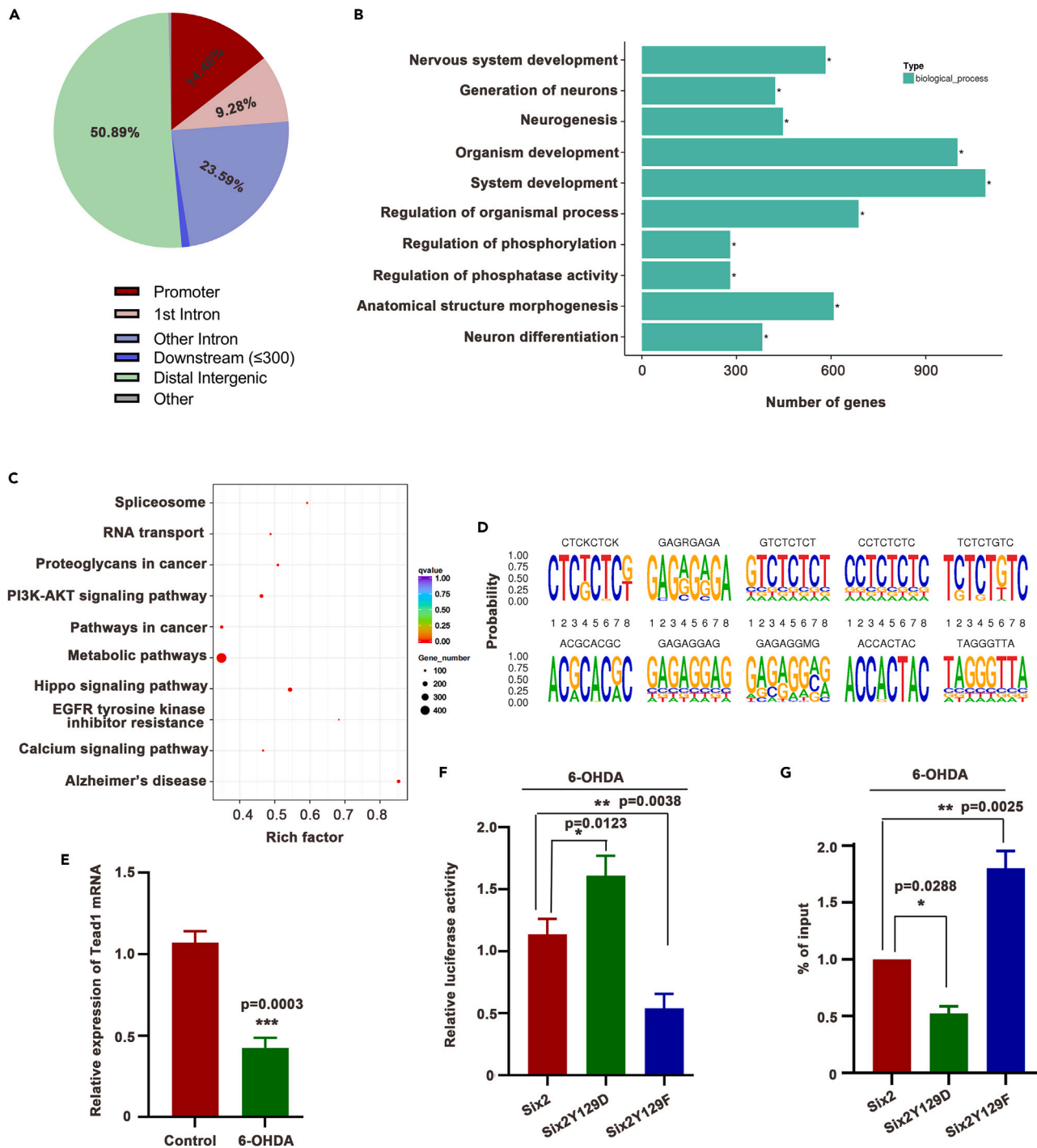


Figure 5. Dephosphorylated Six2 negatively regulates the expression of Tead1 by binding to its promoter

(A) Loci distribution of Six2-bound differential expressed target genes in MES23.5 DA neuron models after treatment with 6-OHDA (100 μ M, 1 h). The word 'down2k' means 2000 bp downstream of the transcription termination site of the genes, 'up2k' means 2000 bp upstream from the transcription start site of the genes, 'exon' means exon region of the genes, 'intron' means intron region of the genes.

(B) GO analysis showed that the cell function distribution of selected proteins that might regulated by Six2.

(C) KEGG analysis showed associated signal pathway that might be regulated by Six2.

(D) Potential candidate motifs prediction of Six2 in MES23.5 DA neuron models after treatment with 6-OHDA (100 μ M, 1h).

(E) qRT-PCR detected the expression of genes in MES23.5 DA neuron models after treatment with 6-OHDA (100 μ M, 1 h).

Figure 5. Continued

(F) Double luciferase reporter gene analysis detects the transcriptional activity of wild-type Six2 and Six2Y129F mutant to Tead1 in DA cells treated with 6-OHDA.

(G) Chromatin immunoprecipitation assay with anti-Six2 antibody for Tead1 in MES23.5 DA cells treated with 6-OHDA (100 μ M, 1 h), ChIP DNA was quantified by qPCR and normalised to input. The statistical analysis was carried out using t tests and one-way ANOVA followed by *post hoc* Newman–Keuls tests. * $p < 0.05$, ** $p < 0.01$ and *** $p < 0.001$; $n = 3$.

Dephosphorylated Six2 inhibited apoptosis of MES23.5 DA cells by downregulating Tead1 expression

We further observed whether dephosphorylated Six2 could protect DA cells by inhibiting the expression of Tead1 *in vitro*. CCK8 analysis revealed that overexpression of Six2Y129F rescued the viability of 6-OHDA treated MES23.5 DA cells; however, Tead1 blocked the protective effect of Six2Y129F when they were co-expressed in MES23.5 DA cells (Figure 6A). Moreover, overexpression of Six2Y129F inhibited the 6-OHDA induced upregulation of bax and downregulation of bcl-2. At the same time, Tead1 reversed the effect of Six2Y129F on the expression of bax and bcl-2 (Figure 6B). In addition, we detected cell apoptosis by TUNEL analysis, the data also demonstrated that Six2Y129F reversed the 6-OHDA induced cell apoptosis, and Tead1 abolished the anti-apoptosis effect of Six2Y129F (Figure 6C). Together, these results indicate that dephosphorylated Six2 could inhibit apoptosis of DA cells by downregulating Tead1 expression.

Dephosphorylated Six2 inhibited the loss of SNpc TH⁺ cells in 6-OHDA-induced PD model rats

The above results strongly supported dephosphorylated Six2 reversed apoptosis of MES23.5 cells by inhibiting Tead1 expression. We wondered whether Six2 and Tead1 signaling prevents the loss of SNpc TH⁺ cells *in vivo*. Therefore, we used a PD model via stereotactic injection of 6-OHDA into the SNpc of rats (Figure 7A). The apomorphine-induced rotation test confirmed that the motor abilities of PD rats were significantly improved in the Six2Y129F group, whereas Tead1 blocked the effect of Six2Y129F (Figure 7B). In addition, the posture asymmetry experiment indicated that the frequency of head turning to the lesioned side improved after Six2Y129F rescue, whereas Tead1 blocked the effect of Six2Y129F (Figure 7C). To further verify the protection of Six2Y129F and Tead1 signaling on damaged DA neurons, the numbers of TH⁺ cells in the SNpc were counted. Results showed that the loss of TH⁺ cells induced by 6-OHDA significantly reduced in Six2Y129F group, and these effects were blocked by co-treatment with Tead1 (Figure 7D). We also examined TH expression in the midbrain and found that Six2Y129F increased the expression of TH, and the effect of Six2Y129F was blocked by Tead1 (Figure 7E). These results suggest that dephosphorylated Six2 significantly protects damaged DA neurons in the SNpc of PD rats by negative regulation of Tead1 expression.

DISCUSSION

PD is a neurodegenerative illness characterized by the selective loss of DA neurons. Previous research has shown that the Six2 transcription factor could protect against DA neurodegeneration in a dephosphorylated form. In this study, we confirmed that the phosphatase Eya1 dephosphorylated Six2 through forming a complex in which Eya1 dephosphorylated Six2 at the tyrosine 129 site in damaged DA neurons, then Six2 translocated from the cytoplasm to the nucleus and inhibited Tead1 expression, reducing damaged DA neuron loss and improving motor function in PD rats.

A previous study has shown that Six2 can directly bind to the Glial cell line-derived neurotrophic factor promoter region to regulate its transcription during kidney development.³¹ Our previous study further demonstrated that Six2 can protect DA cells by promoting Glial cell line-derived neurotrophic factor expression in a low phosphorylation state.¹² In this study, we provided additional evidence that Six2 phosphorylation levels were reduced in DA cells treated with 6-OHDA for 1 h, suggesting that the transcription factor Six2 might exert its transcriptional activity in the dephosphorylation state.

The EYA family protein is a transcriptional cofactor with phosphatase activity, in its transactivation role, a crucial step is an interaction with the SIX family of homeodomain proteins.^{14,30} Although some studies have shown that Eya1 can cooperate with Six2 to transcriptionally activate other target genes,^{32,33} and Eya1 can interact with Six2 and Myc to regulate the expansion of the nephron progenitor pool during nephrogenesis,²³ they do not show that Eya1 can directly combine with Six2 to form a complex. In this study, we provided direct evidence that Eya1 and Six2 are co-expressed in DA cells and can interact to form a complex. Eya1 is a transcriptional cofactor with phosphatase activity, and D327 is the crucial site to determine

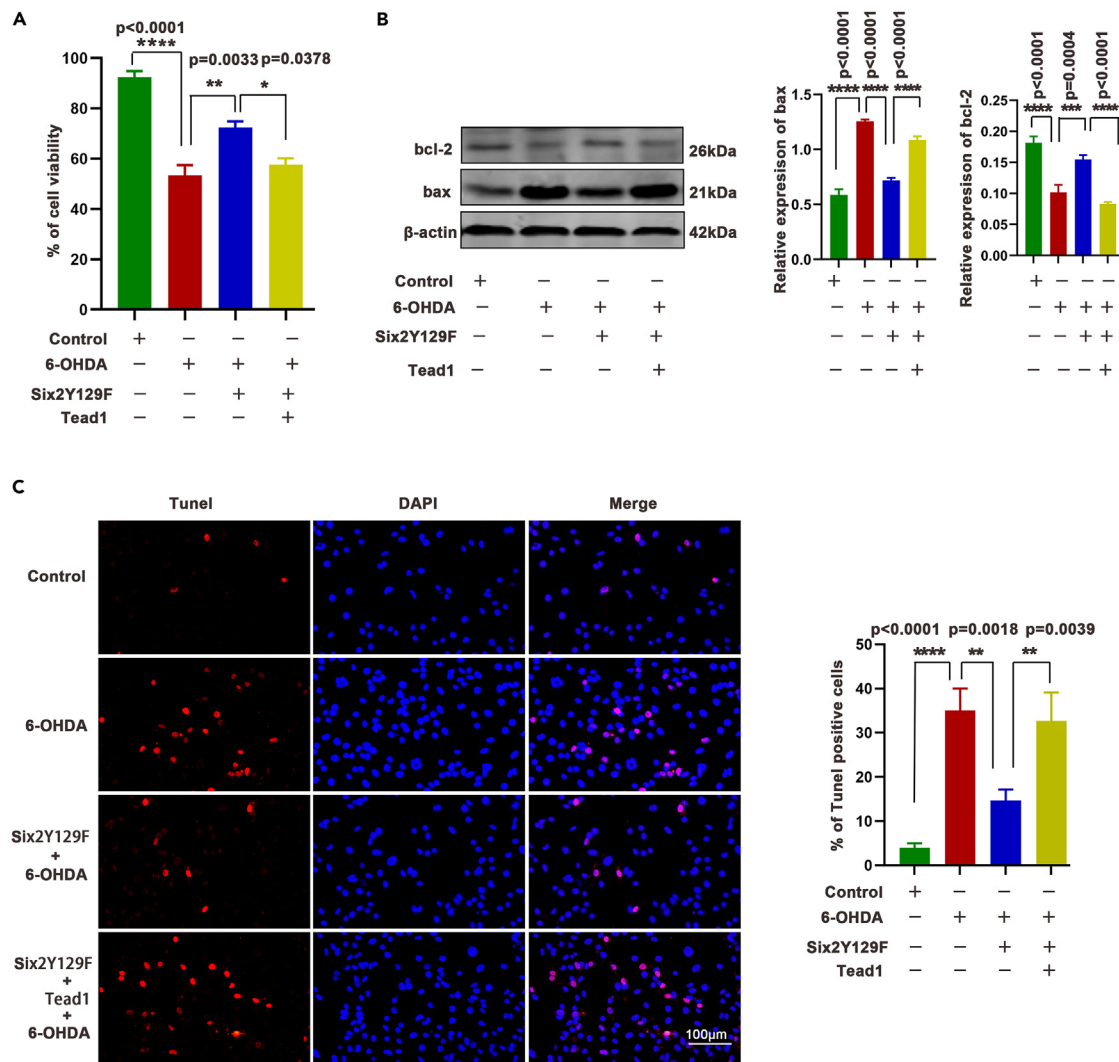


Figure 6. Dephosphorylated Six2 protects MES23.5 DA cells by downregulating Tead1 expression

(A) CCK8 analysis showed the effect of Six2Y129 and Tead1 on cell viability of MES23.5 cells treated with 6-OHDA (100 μ M, 1 h).

(B) IB analysis detects the effect of Six2Y129 and Tead1 on protein expression of Bcl-2 and bax in MES23.5 cells.

(C) TUNEL analysis shows the effect of Six2Y129 and Tead1 on cell apoptosis of MES23.5 cells. The statistical analysis was carried out using one-way ANOVA followed by *post hoc* Newman–Keuls tests. * $p < 0.05$, ** $p < 0.01$, *** $p < 0.001$ and **** $p < 0.0001$; $n = 3$.

the activity of Eya1 phosphatase. In this research, we found that the phosphorylation level of Six2 increased significantly, whereas the phosphatase activity of Eya1 was inactivated by mutating the 327D site to A, and the *in vitro* phosphatase assay further confirmed that Eya1 was the phosphatase of Six2 in injured DA cells. These results suggest that Eya1 is the phosphatase of Six2 in injured DA neurons, it can dephosphorylate Six2 by forming a complex with Six2.

It has been shown that the highly conserved C-terminal domain of the Eya family members contained tyrosine phosphatase activity.^{21,34,35} Although the less conserved N-terminal domain does not contain a sequence motif that shares homology with any other known phosphatase, it has been suggested that the N-terminal domain of Eya members harbors threonine phosphatase activity.^{22,29} Here, we demonstrated that Eya1 dephosphorylated the tyrosine rather than threonine residues of Six2 in damaged DA neurons and identified the Y129 site as the dephosphorylation site of Six2.

With posttranslational modifications, spatial regulation of transcription factors is a common mechanism of altering transcriptional activity. Studies in cultured COS7 cells revealed that vertebrate SIX subgroups are

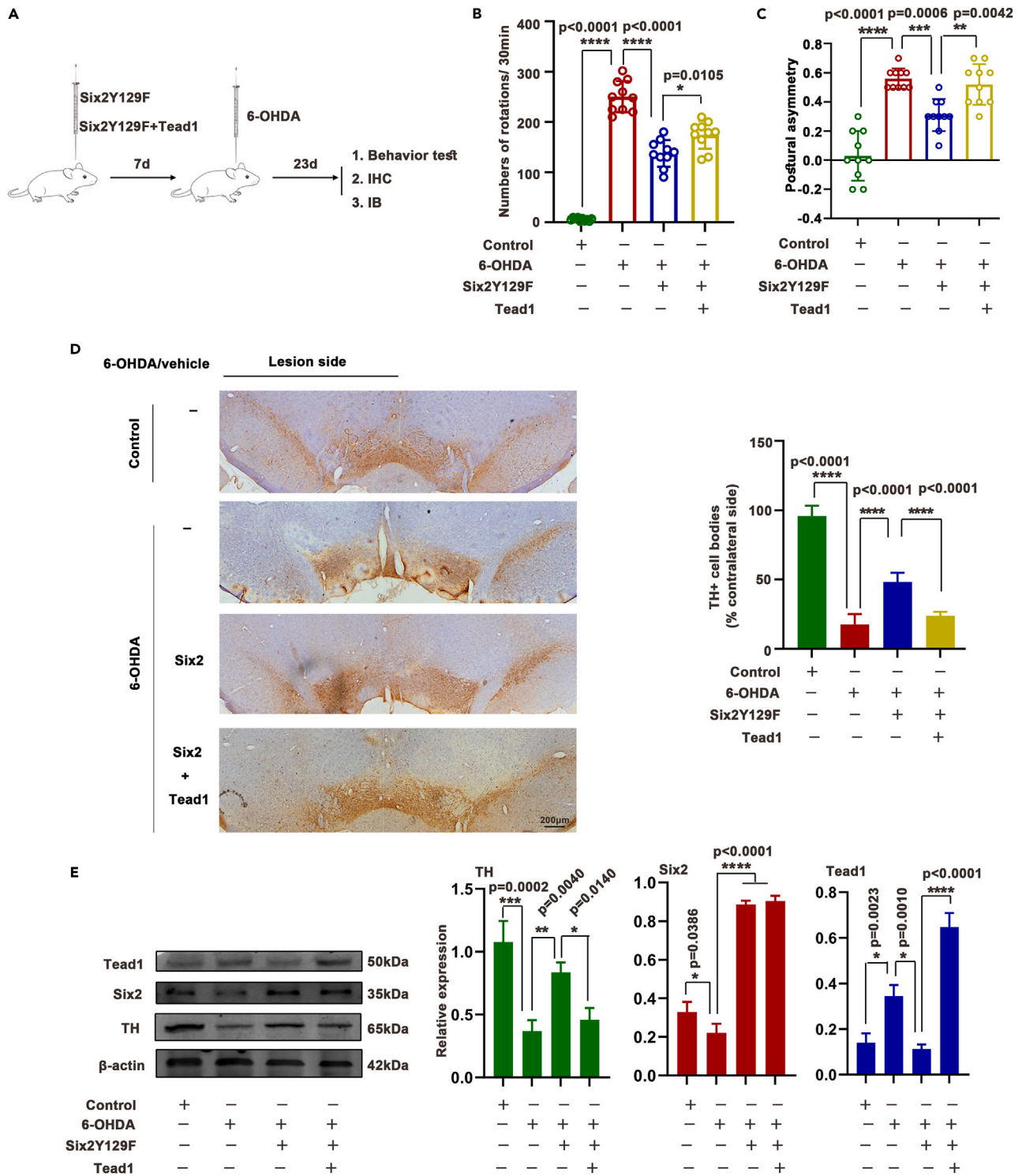


Figure 7. Dephosphorylated Six2 inhibits DA neuronal loss in 6-OHDA-induced PD model rats

(A) The schematic diagram showed the animal experimental procedure and the expression of the virus carrying Six2Y129F in SNpc. (B and C) Results of apomorphine-induced rotation and postural asymmetry of rats in all groups (75 μ g 6-OHDA for 23 days); n = 10.

Figure 7. Continued

(D) Immunohistochemical staining was performed via anti-TH antibody to detect the change of TH⁺ cells, and summarized data showed the total number of TH⁺ cells (% of contralateral side) in the SNpc. Scale bar, 200 μ m. n = 5 per group.

(E) Rat midbrain were isolated and the proteins were collected to measure the protein levels of TH, Six2 and Tead1 in different groups using IB analyses, n = 3. The statistical analysis was carried out using one-way ANOVA followed by *post hoc* Newman–Keuls tests. *p < 0.05, **p < 0.01, ***p < 0.001 and ****p < 0.0001.

located in the nucleus through its nuclear location signal. They could help EYA members translocate into the nucleus.¹⁴ Another report showed that the Abelson tyrosine kinase-mediated phosphorylation relocated EYA from the nucleus to the cytoplasm.³⁶ Other studies have found that cytoplasmic EYA3 tyrosine phosphatase activity promotes cell motility.³⁷ However, the function of the EYA tyrosine phosphatase in DNA repair is nuclear activity.²⁴ Here, we found that phosphorylated Six2 was primarily localized within the cytoplasm, and dephosphorylated Six2 was mainly present in the nucleus, whereas Eya1 was mainly located in the cytoplasm, either in the control group or in the 6-OHDA treatment group. These results suggest that the dephosphorylation of Six2Y129 by Eya1 occurs in the cytoplasm, and this change in Six2 dephosphorylation promotes its translocation from the cytoplasm to the nucleus in DA cells.

The central biological role of the transcription factor is to regulate gene expression. To uncover the precise mechanism of Six2 regulation in injured DA neurons, we performed ChIP-Seq analysis to identify the genome-wide Six2-binding sites, and further KEGG pathway analysis revealed that the Hippo signaling pathway was one of the most significantly enriched pathways, further ChIP-qPCR and luciferase results indicated the Six2 directly regulated the expression of Tead1. TEAD proteins constitute a family of highly conserved transcription factors characterized by a DNA-binding domain called the TEA domain and a protein-binding domain that permits association with transcriptional co-activators. TEAD transcription factors bind to the co-activator YAP/TAZ and regulate the transcriptional output of the Hippo pathway.^{38,39} Hippo is a conserved signaling pathway that regulates the size of organs/tumorigenesis by inhibiting cell proliferation and promoting cell apoptosis.^{40–43} In this study, we found that Tead1 promoted the apoptosis of DA neurons treated with 6-OHDA, and the dephosphorylated Six2 could significantly prevent the apoptotic effect by inhibiting the expression of Tead1. Meanwhile, behavioral results also showed that dephosphorylated Six2 significantly improved the motor ability of PD model rats by negatively regulating the expression of Tead1.

In conclusion, the present study indicates that the dephosphorylation of Six2Y129 by the phosphatase Eya1 is essential for its translocation into the nucleus to regulate Tead1 expression, thereby inhibiting the apoptosis of DA neurons and improving the motor ability of PD model rats. These results reveal a dephosphorylation-dependent mechanism of Six2 that restores the degeneration of DA neurons and provide a potential target to prevent or slow the progressive degeneration of DA neurons in PD.

Limitations of the study

In the present study, we confirmed that the phosphatase Eya1 dephosphorylated Six2 through forming a complex in which Eya1 dephosphorylated Six2 at the tyrosine 129 site in damaged DA cells, then Six2 translocated from the cytoplasm to the nucleus and inhibited Tead1 expression, reversing damaged loss of TH⁺ cells in SNpc and improving motor function in PD rats. However, drug development for Six2 has a long way to go. Moreover, whether these observed anti-PD effects of Six2 in this study could be recapitulated in humans is also unclear. In addition, The DA neurons in the brain are mainly distributed in the SNpc, the ventral tegmental area and the arcuate nucleus of the hypothalamus. However, only the DA neurons in the SNpc have selective vulnerability in PD, and the neurons in SNpc are mainly DA neurons.⁴⁴ TH is a monooxygenase, it is a rate-limiting enzyme that catalyzes organisms synthesize levodopa. Levodopa is the precursor of dopamine, dopamine is the precursor of norepinephrine, and norepinephrine is the precursor of epinephrine. Neurons containing dopamine, norepinephrine and epinephrine are collectively called catecholaminergic neurons. TH is usually used as the specific marker for catecholaminergic neurons.⁴⁵ Although the IHC analysis using TH antibody combined with the location of SNpc was usually used to evaluate DA neurons,^{46–48} in future research, we should consider employing additional markers more specific to DA neurons to validate and extend our findings.

STAR★METHODS

Detailed methods are provided in the online version of this paper and include the following:

- KEY RESOURCES TABLE
- RESOURCE AVAILABILITY

- Lead contact
- Materials availability
- Data and code availability
- **EXPERIMENTAL MODEL AND SUBJECT DETAILS**
 - Experimental cellular models and subject details
 - Experimental animals and ethics
 - SNpc lentivirus injection and PD models construction
- **METHOD DETAILS**
 - Immunoblotting (IB)
 - Cell transfection
 - Immunofluorescence (IF)
 - Co-Immunoprecipitation (Co-IP)
 - GST pull down
 - Protein expression and purification
 - *In vitro* phosphatase assay
 - Real-time polymerase chain reaction (Real-time PCR)
 - Chromatin immunoprecipitation (ChIP)-seq and ChIP-qPCR
 - Dual-luciferase reporter assay
 - Cell viability assay
 - TUNEL staining
 - Immunohistochemistry (IHC) and cell counting
 - Behavioural analysis
- **QUANTIFICATION AND STATISTICAL ANALYSIS**

ACKNOWLEDGMENTS

Many thanks to my colleagues in the department of Neurobiology of Xuzhou Medical University, and the colleagues in the Public Research Center of Xuzhou Medical University.

This work was supported by the Natural Science Foundation of Jiangsu Province (grant number BK20221225), National Natural Science Foundation of China Project (grant number 81901299), Postgraduate Innovation Project of Jiangsu Province (KYCX22_2865), and Scientific Research Project of Affiliated Hospital of Xuzhou Medical University (2021ZA39).

AUTHOR CONTRIBUTIONS

C-T.Z. and J.G. conceived the project and wrote the manuscript. D-L.Q., C-T.Z. designed and performed the major experiments, analyzed data and interpreted the results. X-Y.C., J-S.K., and X-X.H. provided technical support. D-S.G. and J.G. supervised the study, contributed to the conception and design, and helped write and revise the manuscript. All the other authors discussed and formulated the manuscript.

DECLARATION OF INTERESTS

The authors declare no competing interest.

Received: December 25, 2022

Revised: April 3, 2023

Accepted: June 1, 2023

Published: June 7, 2023

REFERENCES

1. Aryal, S., Skinner, T., Bridges, B., and Weber, J.T. (2020). The pathology of Parkinson's disease and potential benefit of dietary polyphenols. *Molecules* 25, 4382. <https://doi.org/10.3390/molecules25194382>.
2. Elsworth, J.D. (2020). Parkinson's disease treatment: past, present, and future. *J. Neural. Transm.* 127, 785–791. <https://doi.org/10.1007/s00702-020-02167-1>.
3. Simon, D.K., Tanner, C.M., and Brundin, P. (2020). Parkinson disease epidemiology, pathology, genetics, and pathophysiology. *Clin. Geriatr. Med.* 36, 1–12. <https://doi.org/10.1016/j.cger.2019.08.002>.
4. Ohto, H., Takizawa, T., Saito, T., Kobayashi, M., Ikeda, K., and Kawakami, K. (1998). Tissue and developmental distribution of Six family gene products. *Int. J. Dev. Biol.* 42, 141–148.
5. Armat, M., Ramezani, F., Molavi, O., Sabzichi, M., and Samadi, N. (2016). Six family of homeobox genes and related mechanisms in tumorigenesis protocols. *Tumori* 2016, 236–243. <https://doi.org/10.5301/tj.5000495>.
6. Kobayashi, A., Valerius, M.T., Mugford, J.W., Carroll, T.J., Self, M., Oliver, G., and McMahon, A.P. (2008). Six2 defines and regulates a multipotent self-renewing

- nephron progenitor population throughout mammalian kidney development. *Cell Stem Cell* 3, 169–181. <https://doi.org/10.1016/j.stem.2008.05.020>.
7. Wang, C.A., Drasin, D., Pham, C., Jedlicka, P., Zaberezhnyy, V., Guney, M., Li, H., Nemenoff, R., Costello, J.C., Tan, A.C., and Ford, H.L. (2014). Homeoprotein Six2 promotes breast cancer metastasis via transcriptional and epigenetic control of E-cadherin expression. *Cancer Res.* 74, 7357–7370. <https://doi.org/10.1158/0008-5472.CAN-14-0666>.
 8. Zheng, L., Guo, Q., Xiang, C., Liu, S., Jiang, Y., Gao, L., Ni, H., Wang, T., Zhao, Q., Liu, H., et al. (2019). Transcriptional factor six2 promotes the competitive endogenous RNA network between CYP4Z1 and pseudogene CYP4Z2P responsible for maintaining the stemness of breast cancer cells. *J. Hematol. Oncol.* 12, 23. <https://doi.org/10.1186/s13045-019-0697-6>.
 9. Lv, X., Mao, Z., Lyu, Z., Zhang, P., Zhan, A., Wang, J., Yang, H., Li, M., Wang, H., Wan, Q., et al. (2014). miR181c promotes apoptosis and suppresses proliferation of metanephric mesenchyme cells by targeting Six2 in vitro. *Cell Biochem. Funct.* 32, 571–579. <https://doi.org/10.1002/cbf.3052>.
 10. Gu, Y., Zhao, Y., Zhou, Y., Xie, Y., Ju, P., Long, Y., Liu, J., Ni, D., Cao, F., Lyu, Z., et al. (2016). Zeb1 is a potential regulator of Six2 in the proliferation, apoptosis and migration of metanephric mesenchyme cells. *Int. J. Mol. Sci.* 17, 1283. <https://doi.org/10.3390/ijms17081283>.
 11. Gao, J., Kang, X.Y., Sun, S., Li, L., Zhang, B.L., Li, Y.Q., and Gao, D.S. (2016). Transcription factor Six2 mediates the protection of GDNF on 6-OHDA lesioned dopaminergic neurons by regulating Smurf1 expression. *Cell Death Dis.* 7, e2217. <https://doi.org/10.1038/cddis.2016.120>.
 12. Gao, J., Kang, X.Y., Sun, S., Li, L., and Gao, D.S. (2020). MES23.5 DA immortalized neuroblastoma cells self-protect against early injury by overexpressing glial cell-derived neurotrophic factor via Akt1/Eya1/six2 signaling. *J. Mol. Neurosci.* 70, 328–339. <https://doi.org/10.1007/s12031-019-01416-7>.
 13. Bonini, N.M., Leiserson, W.M., and Benzer, S. (1993). The eyes absent gene: genetic control of cell survival and differentiation in the developing *Drosophila* eye. *Cell* 72, 379–395. [https://doi.org/10.1016/0092-8674\(93\)90115-7](https://doi.org/10.1016/0092-8674(93)90115-7).
 14. Ohto, H., Kamada, S., Tago, K., Tominaga, S.I., Ozaki, H., Sato, S., and Kawakami, K. (1999). Cooperation of six and eya in activation of their target genes through nuclear translocation of Eya. *Mol. Cell Biol.* 19, 6815–6824. <https://doi.org/10.1128/MCB.19.10.6815>.
 15. Xu, P.X., Adams, J., Peters, H., Brown, M.C., Heaney, S., and Maas, R. (1999). Eya1-deficient mice lack ears and kidneys and show abnormal apoptosis of organ primordia. *Nat. Genet.* 23, 113–117. <https://doi.org/10.1038/12722>.
 16. Stucki, M. (2009). Histone H2A.X Tyr142 phosphorylation: a novel sWItCH for apoptosis? *DNA Repair* 8, 873–876. <https://doi.org/10.1016/j.dnarep.2009.04.003>.
 17. Wu, K., Li, Z., Cai, S., Tian, L., Chen, K., Wang, J., Hu, J., Sun, Y., Li, X., Ertel, A., and Pestell, R.G. (2013). EYA1 phosphatase function is essential to drive breast cancer cell proliferation through cyclin D1. *Cancer Res.* 73, 4488–4499. <https://doi.org/10.1158/0008-5472.CAN-12-4078>.
 18. Kong, D., Ma, W., Zhang, D., Cui, Q., Wang, K., Tang, J., Liu, Z., and Wu, G. (2019). EYA1 promotes cell migration and tumor metastasis in hepatocellular carcinoma. *Am. J. Transl. Res.* 11, 2328–2338.
 19. Roychoudhury, K., and Hegde, R.S. (2021). The eyes absent proteins: unusual HAD family tyrosine phosphatases. *Int. J. Mol. Sci.* 22, 3925. <https://doi.org/10.3390/ijms22083925>.
 20. Li, X., Oghi, K.A., Zhang, J., Krones, A., Bush, K.T., Glass, C.K., Nigam, S.K., Aggarwal, A.K., Maas, R., Rose, D.W., and Rosenfeld, M.G. (2003). Eya protein phosphatase activity regulates Six1-Dach-Eya transcriptional effects in mammalian organogenesis. *Nature* 426, 247–254. <https://doi.org/10.1038/nature02083>.
 21. Rayapureddi, J.P., Kattamuri, C., Steinmetz, B.D., Frankfort, B.J., Ostrin, E.J., Mardon, G., and Hegde, R.S. (2003). Eyes absent represents a class of protein tyrosine phosphatases. *Nature* 426, 295–298. <https://doi.org/10.1038/nature02093>.
 22. Okabe, Y., Sano, T., and Nagata, S. (2009). Regulation of the innate immune response by threonine-phosphatase of Eyes absent. *Nature* 460, 520–524. <https://doi.org/10.1038/nature08138>.
 23. Xu, J., Wong, E.Y.M., Cheng, C., Li, J., Sharkar, M.T.K., Xu, C.Y., Chen, B., Sun, J., Jing, D., and Xu, P.X. (2014). Eya1 interacts with Six2 and Myc to regulate expansion of the nephron progenitor pool during nephrogenesis. *Dev. Cell* 31, 434–447. <https://doi.org/10.1016/j.devcel.2014.10.015>.
 24. Cook, P.J., Ju, B.G., Telese, F., Wang, X., Glass, C.K., and Rosenfeld, M.G. (2009). Tyrosine dephosphorylation of H2AX modulates apoptosis and survival decisions. *Nature* 458, 591–596. <https://doi.org/10.1038/nature07849>.
 25. Krishnan, N., Jeong, D.G., Jung, S.K., Ryu, S.E., Xiao, A., Allis, C.D., Kim, S.J., and Tonks, N.K. (2009). Dephosphorylation of the C-terminal tyrosyl residue of the DNA damage-related histone H2A.X is mediated by the protein phosphatase eyes absent. *J. Biol. Chem.* 284, 16066–16070. <https://doi.org/10.1074/jbc.C900032200>.
 26. Yuan, B., Cheng, L., Chiang, H.C., Xu, X., Han, Y., Su, H., Wang, L., Zhang, B., Lin, J., Li, X., et al. (2014). A phosphotyrosine switch determines the antitumor activity of ERbeta. *J. Clin. Invest.* 124, 3378–3390. <https://doi.org/10.1172/JCI74085>.
 27. Zhang, H., Wang, L., Wong, E.Y.M., Tsang, S.L., Xu, P.X., Lendahl, U., and Sham, M.H. (2017). An Eya1-Notch axis specifies bipotential epibranchial differentiation in mammalian craniofacial morphogenesis. *Elife* 6, e30126. <https://doi.org/10.7554/eLife.30126>.
 28. Merk, D.J., Zhou, P., Cohen, S.M., Pazyra-Murphy, M.F., Hwang, G.H., Rehm, K.J., Alfaro, J., Reid, C.M., Zhao, X., Park, E., et al. (2020). The Eya1 phosphatase mediates Shh-driven Symmetric cell division of cerebellar granule cell precursors. *Dev. Neurosci.* 42, 170–186. <https://doi.org/10.1159/000512976>.
 29. Li, J., Rodriguez, Y., Cheng, C., Zeng, L., Wong, E.Y.M., Xu, C.Y., Zhou, M.M., and Xu, P.X. (2017). EYA1's conformation specificity in dephosphorylating phosphothreonine in Myc and its activity on Myc stabilization in breast cancer. *Mol. Cell Biol.* 37, e00499-16. <https://doi.org/10.1128/MCB.00499-16>.
 30. Xu, P.X. (2013). The EYA-SO/SIX complex in development and disease. *Pediatr. Nephrol.* 28, 843–854. <https://doi.org/10.1007/s00467-012-2246-1>.
 31. Brodbeck, S., Besenbeck, B., and Englert, C. (2004). The transcription factor Six2 activates expression of the Gdnf gene as well as its own promoter. *Mech. Dev.* 121, 1211–1222. <https://doi.org/10.1016/j.mod.2004.05.019>.
 32. Li, J., Xu, J., Jiang, H., Zhang, T., Ramakrishnan, A., Shen, L., and Xu, P.X. (2021). Chromatin remodelers interact with Eya1 and Six2 to target enhancers to control nephron progenitor cell maintenance. *J. Am. Soc. Nephrol.* 32, 2815–2833. <https://doi.org/10.1681/ASN.2021040525>.
 33. Xu, J., Li, J., Ramakrishnan, A., Yan, H., Shen, L., and Xu, P.X. (2022). Six1 and Six2 of the sine Oculis homeobox subfamily are not functionally interchangeable in mouse nephron formation. *Front. Cell Dev. Biol.* 10, 815249. <https://doi.org/10.3389/fcell.2022.815249>.
 34. Tootle, T.L., Silver, S.J., Davies, E.L., Newman, V., Latek, R.R., Mills, I.A., Selengut, J.D., Parlikar, B.E.W., and Rebay, I. (2003). The transcription factor Eyes absent is a protein tyrosine phosphatase. *Nature* 426, 299–302. <https://doi.org/10.1038/nature02097>.
 35. Jemc, J., and Rebay, I. (2007). Identification of transcriptional targets of the dual-function transcription factor/phosphatase eyes absent. *Dev. Biol.* 310, 416–429. <https://doi.org/10.1016/j.ydbio.2007.07.024>.
 36. Xiong, W., Dabbouseh, N.M., and Rebay, I. (2009). Interactions with the Abelson tyrosine kinase reveal compartmentalization of eyes absent function between nucleus and cytoplasm. *Dev. Cell* 16, 271–279. <https://doi.org/10.1016/j.devcel.2008.12.005>.
 37. Pandey, R.N., Rani, R., Yeo, E.J., Spencer, M., Hu, S., Lang, R.A., and Hegde, R.S. (2010). The Eyes Absent phosphatase-transactivator proteins promote proliferation, transformation, migration, and invasion of tumor cells. *Oncogene* 29, 3715–3722. <https://doi.org/10.1038/onc.2010.122>.
 38. Landin-Malt, A., Benhaddou, A., Zider, A., and Flagiello, D. (2016). An evolutionary,

- structural and functional overview of the mammalian TEAD1 and TEAD2 transcription factors. *Gene* 591, 292–303. <https://doi.org/10.1016/j.gene.2016.07.028>.
39. Lin, K.C., Park, H.W., and Guan, K.L. (2017). Regulation of the Hippo pathway transcription factor TEAD. *Trends Biochem. Sci.* 42, 862–872. <https://doi.org/10.1016/j.tibs.2017.09.003>.
 40. Lapi, E., Di Agostino, S., Donzelli, S., Gal, H., Domany, E., Rechavi, G., Pandolfi, P.P., Givol, D., Strano, S., Lu, X., and Blandino, G. (2008). PML, YAP, and p73 are components of a proapoptotic autoregulatory feedback loop. *Mol. Cell* 32, 803–814. <https://doi.org/10.1016/j.molcel.2008.11.019>.
 41. Cottini, F., Hideshima, T., Xu, C., Sattler, M., Dori, M., Agnelli, L., ten Hacken, E., Bertilaccio, M.T., Antonini, E., Neri, A., et al. (2014). Rescue of Hippo coactivator YAP1 triggers DNA damage-induced apoptosis in hematological cancers. *Nat. Med.* 20, 599–606. <https://doi.org/10.1038/nm.3562>.
 42. Yu, F.X., Zhao, B., and Guan, K.L. (2015). Hippo pathway in organ size control, tissue homeostasis, and cancer. *Cell* 163, 811–828. <https://doi.org/10.1016/j.cell.2015.10.044>.
 43. Masliantsev, K., Karayan-Tapon, L., and Guichet, P.O. (2021). Hippo signaling pathway in gliomas. *Cells* 10, 184. <https://doi.org/10.3390/cells10010184>.
 44. Gonzalez-Rodriguez, P., Zampese, E., and Surmeier, D.J. (2020). Selective neuronal vulnerability in Parkinson's disease. *Prog. Brain Res.* 252, 61–89. <https://doi.org/10.1016/bs.pbr.2020.02.005>.
 45. Pearson, J., Goldstein, M., Markey, K., and Brandeis, L. (1983). Human brainstem catecholamine neuronal anatomy as indicated by immunocytochemistry with antibodies to tyrosine hydroxylase. *Neuroscience* 8, 3–32. [https://doi.org/10.1016/0306-4522\(83\)90023-4](https://doi.org/10.1016/0306-4522(83)90023-4).
 46. Yu, H., Liu, X., Chen, B., Vickstrom, C.R., Friedman, V., Kelly, T.J., Bai, X., Zhao, L., Hillard, C.J., and Liu, Q.S. (2021). The neuroprotective effects of the CB2 Agonist GW842166x in the 6-OHDA mouse model of Parkinson's disease. *Cells* 10, 3548. <https://doi.org/10.3390/cells10123548>.
 47. Choi-Lundberg, D.L., Lin, Q., Chang, Y.N., Chiang, Y.L., Hay, C.M., Mohajeri, H., Davidson, B.L., and Bohn, M.C. (1997). Dopaminergic neurons protected from degeneration by GDNF gene therapy. *Science* 275, 838–841. <https://doi.org/10.1126/science.275.5301.838>.
 48. Lindholm, P., Voutilainen, M.H., Laurén, J., Peränen, J., Leppänen, V.M., Andressoo, J.O., Lindahl, M., Janhunen, S., Kalkkinen, N., Timmusk, T., et al. (2007). Novel neurotrophic factor CDNF protects and rescues midbrain dopamine neurons in vivo. *Nature* 448, 73–77. <https://doi.org/10.1038/nature05957>.
 49. Borlongan, C.V., Saporta, S., Poulos, S.G., Othberg, A., and Sanberg, P.R. (1998). Viability and survival of hNT neurons determine degree of functional recovery in grafted ischemic rats. *Neuroreport* 9, 2837–2842. <https://doi.org/10.1097/00001756-199808240-00028>.
 50. Chang, C.F., Lin, S.Z., Chiang, Y.H., Morales, M., Chou, J., Lein, P., Chen, H.L., Hoffer, B.J., and Wang, Y. (2003). Intravenous administration of bone morphogenetic protein-7 after ischemia improves motor function in stroke rats. *Stroke* 34, 558–564. <https://doi.org/10.1161/01.str.0000051507.64423.00>.

STAR★METHODS

KEY RESOURCES TABLE

REAGENT or RESOURCE	SOURCE	IDENTIFIER
Antibodies		
Rabbit monoclonal anti-SIX2	Abcam	Cat# EPR4824; RRID: AB_10862450
Mouse monoclonal anti-SIX2	Santa Cruz, St. Louis	Cat# sc-377193
Rabbit polyclonal anti-phosphoserine/ threonine/tyrosine	Sigma-Aldrich	Cat# 61-8300
Rabbit polyclonal anti-phosphothreonine	Abcam	Cat# ab9337; RRID: AB_307187
Rabbit anti-phospho-Tyrosine	Cell Signaling Technology	Cat# 8954; RRID: AB_2687925
Rabbit polyclonal anti-Eya1	Proteintech	Cat# 22658-1-AP; RRID: AB_2879145
Rabbit polyclonal anti-HA	Proteintech	Cat# 51064-2-AP; RRID: AB_11042321
Rabbit polyclonal anti-Lamin B1	Proteintech	Cat# 12987-1-AP; RRID: AB_2136290
Rabbit polyclonal anti- β -tubulin	Proteintech	Cat# 10068-1-AP; RRID: AB_2303998
Rabbit polyclonal anti- Bax	Proteintech	Cat# 50599-2-Ig; RRID: AB_2061561
Rabbit polyclonal anti- Bcl-2	Proteintech	Cat# 26593-1-AP
Rabbit polyclonal anti-TH	Proteintech	Cat# 25859-1-AP; RRID: AB_2716568
Mouse monoclonal anti- β -actin	Proteintech	Cat# 66009-1-Ig; RRID: AB_2782959
Bacterial and virus strains		
pLV-EGFP:T2A:Puro-SIX2	Yunzhou Biotechnology	N/A
pLV[shSIX2]-EGFP/Puro-U6	Yunzhou Biotechnology	N/A
pLV-EGFP:T2A:Puro-EYA1	Yunzhou Biotechnology	N/A
pLV-EGFP:T2A:Puro-EYA1 D327A	Yunzhou Biotechnology	N/A
pLV-EGFP:T2A:Puro-SIX2 Y67F	Yunzhou Biotechnology	N/A
pLV-EGFP:T2A:Puro-SIX2 Y92F	Yunzhou Biotechnology	N/A
pLV-EGFP:T2A:Puro-SIX2 Y109F	Yunzhou Biotechnology	N/A
pLV-EGFP:T2A:Puro-SIX2 Y129F	Yunzhou Biotechnology	N/A
pLV-EGFP:T2A:Puro-SIX2 Y143F	Yunzhou Biotechnology	N/A
pLV-EGFP:T2A:Puro-SIX2 Y148F	Yunzhou Biotechnology	N/A
pLV-EGFP:T2A:Puro-SIX2 Y129D	Yunzhou Biotechnology	N/A
pLV-EGFP:T2A:Puro-TEAD1	Yunzhou Biotechnology	N/A
Chemicals, peptides, and recombinant proteins		
Phosphorylated peptides	Sangon Biotech	N/A
TRIzol	Vazyme	Cat# R401-01
HiScript II Q Select RT SuperMix for qPCR	Vazyme	Cat# R232-01
AceQ qPCR SYBR Green Master Mix	Vazyme	Cat# R111-02
NaCl	Beyotime Biotechnology	Cat# ST347
KCl	Beyotime Biotechnology	Cat# ST345
MgCl ₂	Beyotime Biotechnology	Cat# ST269
ETDA	Beyotime Biotechnology	Cat# C0196
DTT	Beyotime Biotechnology	Cat# ST041
Critical commercial assays		
ChIP Assay Kit	Beyotime Biotechnology	Cat# P2078
Dual-Lumi™ Luciferase Reporter Gene Assay kit	Beyotime Biotechnology	Cat# RG088S

(Continued on next page)

Continued		
REAGENT or RESOURCE	SOURCE	IDENTIFIER
CCK-8 Kit	Vicmed	Cat# C0038
TUNEL Kit	Vazyme	Cat# A113-01/02/03
Experimental models: Cell lines		
MES23.5 cells	Shanghai Institutes for Cell Resource Center at the Chinese Academy of Sciences	N/A; RRID:CVCL_J351
MN9D cells	Shanghai Institutes for Cell Resource Center at the Chinese Academy of Sciences	N/A; RRID:CVCL_M067
293T cells	Shanghai Institutes for Cell Resource Center at the Chinese Academy of Sciences	N/A; RRID:CVCL_XY89
Experimental models: Organisms/strains		
Male Sprague Dawley rats	Gempharmatech Co., Ltd	Strain NO.D000017
Oligonucleotides		
Primers for <i>Tead1</i> : Forward: TCATCTTATCAGACGAAGGCAA; Reverse: CAGCTTGGAATGAAAATCACGA	This paper	N/A
Primers for β -actin: Forward: CACCCGCGAGTACAACCTTC; Reverse: CCCATACCCACCATCACACC	This paper	N/A
Primers for ChIP-qPCR: Forward: CGTACAGGCCGAGGAGTTAT; Reverse: CCTTCAGACTCCAGTTGCTCC	This paper	N/A
shRNA targeting sequence: SIX2: GCTACTGCTCAAGGAAAA	This paper	N/A
Recombinant DNA		
Plasmid: pGL3-Tead1	Sangon Biotech	N/A
Plasmid: Six2	Sangon Biotech	N/A
Plasmid: Six2 Y129F	Sangon Biotech	N/A
Software and algorithms		
ImageJ	National Institutes of Health MathWorks	https://imagej.nih.gov/ij/ ; RRID:SCR_003070
SPSS	IBM.Lnc.	https://www.ibm.com/cn-zh/spss/ ; RRID:SCR_002865
GraphPad Prism 9	GraphPad Software.Lnc.	http://www.graphpad.com/ ; RRID:SCR_002798

RESOURCE AVAILABILITY

Lead contact

Further information and requests for resources and reagents should be directed to and will be fulfilled by the lead contact, Jin Gao (gaojin@xzhmu.edu.cn).

Materials availability

This study did not generate new unique reagents.

Data and code availability

- All data reported in this paper will be shared by the [lead contact](#) upon request.
- This paper does not report original code.

- Any additional information required to reanalyze the data reported in this paper is available from the [lead contact](#) upon request

EXPERIMENTAL MODEL AND SUBJECT DETAILS

Experimental cellular models and subject details

The MES23.5 and MN9D DA cell lines, and 293T cells were obtained from the Shanghai Institutes for Cell Resource Center at the Chinese Academy of Sciences (Shanghai, China). All cell lines were cultured in Dulbecco's modified Eagle's medium (DMEM/High) supplemented with 10% foetal bovine serum (Hyclone, Logan, UT, USA) and penicillin/streptomycin (PS) (Beyotime Biotechnology, Shanghai, China) in a 5% CO₂ atmosphere at 37°C. The 6-OHDA (H116) were purchased from Sigma (St. Louis, MO, USA). Cell lines were treated with 6-OHDA (100 μM) for different times (30 min, 1 h, 3 h).

Experimental animals and ethics

Adult male Sprague Dawley rats (230–250 g) were provided by Xuzhou Medical University. These rats were housed under controlled conditions (temperature 23 ± 2 °C and illumination 12:12 h light–dark cycle) with standard diet and water *ad libitum*. Animal housing and treatment of the rats were performed in accordance with the Guidelines of the Ethical Committee for the Use of Laboratory Animals.

SNpc lentivirus injection and PD models construction

The Rats were anaesthetized by pentobarbital (50 mg/kg) and then injected with 2 μL virus which were purchased from Shanghai Genechem Co.,Ltd. (Shanghai, China) or an equal volume of PBS to the left SNpc (anteroposterior (AP) -5.2 mm, lateral (LAT) -1 mm and dorsoventral (DV) -8 mm). One week later, 6-OHDA was injected into the same site to construct the PD model.

The rats were divided into 4 groups (10 rats/group): (i) Control group: the rats received left SNpc injection of empty virus and vehicle (0.1% ascorbate in 0.9% saline); (ii) 6-OHDA group: the rats received left SNpc injection of empty virus and 6-OHDA (3 μL, 25 μg/μL); (iii) 6-OHDA+Six2Y129F group: the rats received left SNpc injection of virus containing Six2Y129F and 6-OHDA; (iv) 6-OHDA+Six2Y129F+Tead1: the rats received left SNpc injection of virus containing Six2 and Tead1 and 6-OHDA. Twenty-three days after the 6-OHDA injection, rats in every group were subjected to behavioural tests, and then, these rats were anaesthetised with sodium pentobarbital and transcardially perfused for immunohistochemistry and IB analyses.

METHOD DETAILS

Immunoblotting (IB)

Total protein from the tissue samples and cell lines was extracted. Equal amounts of protein were separated by sodium dodecyl sulphate/polyacrylamide gel electrophoresis and then transferred onto nitrocellulose membranes (Bio-Rad, Hercules, CA, USA). Membranes were blocked for 1 hour with 5% non-fat dry milk (Solarbio, Beijing, China) in Tris-HCl-buffered saline solution containing Tween-20, and then incubated with primary antibodies overnight at 4°C. The primary antibodies included anti-SIX2 Rabbit antibody (Abcam, Cambridge, UK), anti-Phosphoserine/threonine/tyrosine antibody (Sigma-Aldrich, St. Louis, USA), anti-Phosphothreonine antibody (Abcam, Cambridge, UK), anti-Eya1 antibody (Proteintech, Wuhan, China), anti-HA antibody (Proteintech, Wuhan, China), anti-Phospho-Tyrosine antibody (Cell Signaling Technology, Boston, USA), anti-Lamin B1 antibody, anti-β-tubulin antibody (Proteintech, Wuhan, China), anti-Bax antibody, anti-Bcl-2 antibody, anti-TH antibody (Proteintech, Wuhan, China), and anti-β-actin antibody (Proteintech, Wuhan, China). After washing, the specific blots were incubated with a fluorescent secondary antibody (LI-COR, Lincoln, USA) for 2h at room temperature. Blots were detected by Odyssey CLX infrared laser imaging system (LI-COR, Lincoln, USA). β-actin was used as control, and data was quantified by ImageJ Software (National Institutes of Health, Bethesda, MD, USA).

Cell transfection

The lentivirus carrying Six2 (Six2Y67F, Six2Y92F, Six2Y109F, Six2Y129F, Six2Y143F, Six2Y148F, Six2Y129D or Tead1) was purchased from Yunzhou Biotechnology Co., Ltd (Guangzhou, China). Lentiviruses were transfected into MES23.5 DA cells according to the manufacturer's instructions, selected with puromycin

(2 µg/mL, Meilunbio, Dalin, China) after 72 h of transfection and then established the MES23.5 DA cells stably expressing Six2 (or Six2Y129F, Six2Y129D or Tead1).

Immunofluorescence (IF)

MES23.5 DA cells were cultured into 24-well plate slides. When the cells reached 70% confluence, the slides were fixed with 4% paraformaldehyde for 20 min. Washing the slides 3 times, 0.2% Triton X-100 (prepared in PBS) was permeabilized at room temperature for 10 min. The slides were blocked with 5% BSA and 0.3% Triton X-100 for 1 h and incubated with primary antibodies overnight at 4 °C. Primary antibodies included anti-Eya1 antibody (Proteintech, Wuhan, China), anti-SIX2 antibody (Santa Cruz, St. Louis, MO, USA). After washing three times with PBS, the sections were then incubated with Alexa Fluor 488-conjugated donkey anti-rabbit secondary antibody (1:400, Jackson ImmunoResearch Inc, Pennsylvania, USA) and Alexa Fluor 594-conjugated donkey anti-mouse secondary antibody (1:400, Jackson ImmunoResearch Inc, Pennsylvania, USA) at room temperature for 2 h and stained with DAPI (Beyotime Biotechnology, Shanghai, China). Mounting the slide with mounting solution containing anti-fluorescence quencher, and fluorescent images were captured using a laser scanning confocal microscope (Leica STELLARIS 5, Germany). The proportion of Six2 puncta in cytoplasm and nucleus were analysed by image J.

Co-Immunoprecipitation (Co-IP)

Adding 400 µL of diluted antibody to the protein which we extract from cells, and incubating them in an inversion mixer overnight at 4 °C. Another day, 25–50 µL of magnetic beads (MCE, New Jersey, USA) were prepared and mixed with antigen-antibody complex in a 1.5 mL EP tube (4°C, 4 h). Separating the magnetic beads, discarding the supernatant and washing four times. Adding 25–50 µL 1×SDS-PAGE Loading Buffer to the magnetic beads, mix well, and heat at 95°C for 5 min. Separating the magnetic beads. Collecting the supernatant, and performing SDS-PAGE detection.

GST pull down

The vector pGEX-4T-1 was used to express EYA1. GST-tagged EYA1 were expressed in BL21 cells and then purified with a GST protein interaction pull-down Kit. HEK-293T cells over-expressing His-tagged SIX2 protein in vector pcDNA3.1 were lysed in homogenization buffer. The GST pull-down experiment was performed according to the manufacturer's instructions. Briefly, GST-tagged protein (200 µL) was incubated with the pre-equilibrated resin (henghuibio, Beijing, China) at 4°C for 2 h on a rotating platform. After washing five times in TBS containing the pull-down lysis buffer, the SIX2 was co-incubated with GST-tagged protein for 2 h. Finally, the bound proteins were eluted and subjected to IB analysis.

Protein expression and purification

Full-length Eya1 wild-type and mutant D327A protein in a His-fusion format were expressed in 293 cells. The Ni Sepharose 6 Fast Flow (henghuibio, Beijing, China) was pretreated to make it at the same PH value. Add the protein supernatant, which was collected by RIPA buffer into the purified filler to fully mix it, and use 20 mM imidazole solution (BBI Life Sciences Corporation, Shanghai, China) to wash off the impurities combined on the protein purification filler. At last, 200 mM imidazole solution was added to elute the purified protein. Purified Eya1 and mutant D327A protein were concentrated to 1 mg/mL and frozen by liquid nitrogen for long-term storage.

In vitro phosphatase assay

Tyrosine phosphorylated peptides were custom synthesized by Sangon Biotech (Shanghai, China), the peptide sequence of Six2 was GEETSYCFKEKS, and the sequence of H2AX was GPKAPSGGKKATQASQRY. All peptides were purified by high-performance liquid chromatography, and all purified products were analyzed by mass spectrometry. The purity of each peptide was greater than 95%. Purified Eya1 protein (400 ng) was incubated in a final volume of 20 µL with 1 mM peptide in a buffer containing 60 mM HEPES (Beyotime Biotechnology, Shanghai, China), 75 mM NaCl (Beyotime Biotechnology, Shanghai, China), 75 mM KCl (Beyotime Biotechnology, Shanghai, China), 5 mM MgCl₂ (Beyotime Biotechnology, Shanghai, China), 1 mM EDTA (Beyotime Biotechnology, Shanghai, China), and 1 mM DTT (Beyotime Biotechnology, Shanghai, China) at 37°C for 2 h. The released phosphate was quantified using the Malachite Green Phosphate Assay Kit (Sigma-Aldrich, St. Louis, USA). Duplicate values were background corrected and compared to the internal phosphate standard.

Real-time polymerase chain reaction (Real-time PCR)

The cultured MES23.5 cells were harvested and the As described previously (Gao et al. 2020), total RNA from MES23.5 cell lines was extracted using high pure RNA isolation kits (Roche Applied Science, Indianapolis, IN, USA). Then, the RNA was reversely transcribed to cDNA using a transcriptor first-strand cDNA synthesis kit (Roche Applied Science). The expression of *Six2* and *TH* genes was assayed using the SYBR green PCR master mix (Roche Applied Science). The mRNA data were normalised to β -actin. The primers were as follows:

Tead1 (Forward): 5'-TCATCTTATCAGACGAAGGCAA-3',

(Reverse): 5'-CAGCTTGGAATGAAAATCACGA-3';

β -actin (forward): 5'-CACCCGCGAGTACAACCTTC-3',

(reverse): 5'-CCCATACCCACCATCACACC-3'.

Chromatin immunoprecipitation (ChIP)-seq and ChIP-qPCR

ChIP Assay Kit was obtained from Beyotime Biotechnology (Shanghai, China). The experiment was performed according to the manufacturer's instructions. MES23.5 DA cells were treated with 6-OHDA (100 mM) for 1 h. After treatment, cells were fixed in 1% formaldehyde for 10 min, followed by quenching with glycine and rinsing with cold PBS. Afterwards, cell nuclei were released and sonicated into 200-700 base pair (bp) DNA fragments. Aliquots of chromatin were incubated overnight with 5 mg anti-Six2 antibody or control rabbit immunoglobulin G (Proteintech, Wuhan, China). The chromatin-antibody complexes were pulled down with prewashed magnetic beads (MCE, New Jersey, USA), then washed and eluted. DNA fragments associated with Six2 or control antibodies were eluted and purified. Input genomic DNA was obtained through similar elution and purification procedures. Prepared DNA was processed for ChIP-seq or ChIP-qPCR. Real-time qPCRs were performed with the primer pairs as follows:

Tead1 (Forward), 5'-CGTACAGCCGAGGAGTTAT-3';

(Reverse), 5'-CCTTCAGACTCCAGTTGCTCC-3'.

Dual-luciferase reporter assay

Dual-LumiTM Luciferase Reporter Gene Assay kit was obtained from Beyotime Biotechnology (Shanghai, China). The promoter region (-2000bp) of the rat *Tead1* gene was subcloned into pGL3 Basic luciferase reporter plasmid (Promega, Madison, USA). Plasmids carrying the *Six2* and *Six2Y129F* plasmids were transfected into MES23.5 DA cells. After 24 h, the cells were treated with 100 μ M 6-OHDA for 1 h. Luciferase assays were then performed using the Dual-Luciferase Reporter Assay System according to the manufacturer's instructions (Promega). Luciferase activity was measured using an LB940 Multilabel Reader (Berthold Technologies, Bad Wildbad, Germany).

Cell viability assay

Cells were cultured into 96-well plates. After 24 h of incubation, cells were treated with 6-OHDA (100 μ M) for 1 h. After that, 10 μ L CCK-8 (Vicmed, Xuzhou, China) was added to the culture medium, and the viability of the cells was measured 2 h later at 450 nm using a multimode reader (Synergy 2) according to the manufacturer's instructions.

Tunel staining

Apoptosis of MES23.5 cells was detected by TUNEL (Vazyme, Nanjing, China). MES23.5 cells were plated in 24-well plates. After treating with 6-OHDA (100 μ M) for 1 h, detecting cellular apoptosis according to the manufacturer's protocol. The labeled apoptotic cells may be visualized by fluorescence microscopy (Olympus Co., Japan). The apoptosis rate was obtained by dividing the number of blue cells stained by DAPI.

Immunohistochemistry (IHC) and cell counting

The sections were incubated with 10% donkey serum albumin containing 0.3% Triton X-100 for 1 h to block non-specific binding, and then incubated with anti-TH antibody (Proteintech, Wuhan, China) overnight. After washing three times, the rabbit two-step detection kit (OriGene, Wuxi, China) was used for subsequent staining. Then these sections were cleared in xylene, and cover-slipped with cytooseal for observation under a microscope. The sections were imaged with the Olympus cellSens Entry and analyzed by ImageJ software. The first sampling item was taken at random from the frontal part of the SNpc, and every sixth section (20 μ m thickness) was selected. For DA neuron quantification, tyrosine hydroxylase-positive (TH⁺) neurons in the SNpc were counted from both brain heisispheres coronal sections from each rat between approximately -4.7 and -6.3 mm from bregma. The SNpc was carefully outlined to exclude other subdivisions of the SNpc and the ventral tegmental area. TH⁺ neurons were counted only when present completely or partially inside the frame. Counts of DA neurons were expressed as the percentage of contralateral side. We compared the cell number differences within the same slices (control and lesion sides) and between different treatment groups, which minimized potential sampling errors.

Behavioural analysis

The following behavioural tests were carried out 23 days after the 6-OHDA injection for screening the PD rats, and for detecting the effect of Six2Y129F on PD rats.

Postural asymmetry: Postural asymmetry was analysed using the elevated body swing test.^{49,50} The rats were examined for lateral movements with their bodies suspended by their tail 10 cm above the testing table. The frequency of head turning contralateral to the lesioned side (ipsilateral side) was evaluated in 20 continuous trials. The computing method was: (contralateral turns – ipsilateral turns)/total turns.

Apomorphine-induced rotation analysis: Contralateral rotations of each rat were recorded after subcutaneous injection of apomorphine (0.5 mg/kg in normal saline containing 0.01% ascorbic acid) to confirm the dopamine depletion in the nigrostriatal system. The rotation behaviour was counted over a period of 30 min.

QUANTIFICATION AND STATISTICAL ANALYSIS

All data were processed with SPSS 13.0 (SPSS Inc., Chicago, IL, USA). Bar graphs are shown as means \pm S.E.M. Difference was carried out using t-test to compare two independent samples, and one-way analyses of variance (ANOVAs) followed by *post hoc* Newman–Keuls tests to compare all pairs of groups or *post hoc* Dunnett's tests for comparing all experimental groups with the control group. $P < 0.05$ was considered statistically significant for all tests.